A simple Human Simulating Intelligent PID for wind turbine Control under wind speed variation

Abdelhaq Amar bensaber[1], Mustapha Benghanem[1], Abdelmadjid Guerouad[2], Mohammed Amar bensaber[2]

[1]University of Sciences and Technology of Oran

Email:abs.abdelhak@gmail.com, mbenghanem6@yahoo.fr, a.guerouad@yahoo.com.

[2]School of Computer Science 08 May 1945 Sidi Bel Abbès

E-mail : m.amarbensaber@esi-sba.dz

Abstract—**DFIG is an attractive solution in variable wind turbines[1, 2] because of its features like lessening losses, minimum cost, an improved efficiency and power control capabilities[2].Traditionally their control is founded on PID controller because it's simple ,robust which is advisable for linear systems. . However, wind turbines components work as nonlinear systems where electromechanical parameters change frequently [3],. Inspired by the PID simplicity, a Human Simulating Intelligent PID is suggest to contribute with some important features like simplicity, flexibility, self-learning and heftiness, ameliorate respond time, dealing with grid requirements. Matlab tests are introduced and compared.**

Keywords-component; HIS-PID, fed induction generator (DFIG).Active and Reactive Power control, Maximum power point tracking, MPPT.

I. INTRODUCTION

Nowadays, energy production is moving towards the clean and inexhaustible energy because of the desire to reduce reliance on fossil fuels and the global warming issues. Wind energy treated as a future technology because it cost efficiency and reliability [4, 5]. Thus, those factors became important topics in industry and research [6, 7].Control strategies are necessary to attain maximum performance. The DFIG WTs has been an attractive choice [8, 9] because of to the independent power control plus it ability to deal with variable speed due to control of back-to-back converter scheme[10, 11], reduced mechanical stresses[2], recompense for power pulsations and torque [12] and improve power quality[2] ,the major feature of proposed generator is that the power converter is sized between "20–30%" of entire power which means the cost is reduced[13], still the generator respond to voltage disturbances is critical, as expressed in [2, 14] , ,to protect and remain connected to the network even with faults it is required to control the rotor converter. [2, 14-16], the control schemes are established with the vector control with the classical controller, but this controller can provide favorable performance restrictive under ideal voltage conditions. Furthermore, disturbances and parameter variations will leave us with imperfect performance. Therefore, papers have offered many control strategies for DFIG like Sliding Mode Control, smart control or adaptive algorithms [1, 17, 18], HOSMC [6, 15, 16, 19, 20].In this paper we used a simple and practicable control law named Human-Simulating Intelligent PID control; the main goal of

HSIC is how controller itself simulates expert's behavior. Therefore, the system gain can be adjusted according to system output. The HSIC has the advantages of simple construction, quick response, strong anti-interference and strong robustness [21-23].

This article arranged as follows; turbine model and the MPPT are given in the second section. In part III, DFIG mathematical model is introduced. Section IV introduces DFIG Vector Control. In section V HIS-PID controller is proposed. At last, matlab results are given and debated.

II. MODEL OF THE TURBINE:

The power contained in kinetic energy form at a speed V_v, surfaceA_1, is expressed by[14]:

$$P_v = \frac{1}{2} \rho A_1 V_v^3 \qquad (1)$$

Where ρ is the air density, but WT can regain just a part of that power:

$$P_v = \frac{1}{2} \rho \pi R^2 V_v^3 C_p \qquad (2)$$

Where: R is the radius; Cp is power coefficient [24], this coefficient is a related with the wind and wind turbine rotation pace and the pitch angle. The speed ratio λ introduced by:

$$\lambda = \frac{R\Omega_t}{V_v} \qquad (3)$$

Where R is the blades length, Ω_t is the rotor angular speed. The theoretical extreme rate of C_p is given by the Betz limit:
$$C_{p\_theo\_max} = 0,593 = 59,3\%$$

The torque and power coefficient C_p is represented in function of tip step ratio (λ) and the pitch angle (β) as fellow:

$$C_p = C_1(\frac{C_2}{\lambda_i} - C_3\beta - C_4\beta^{C_5} - C_6)(e^{C_7/\lambda_i}) \qquad (4)$$

$$\lambda_i = \frac{1}{\lambda + C_8} \qquad (5)$$

The slow shaft mechanical torque C_t is expressed by:

$$C_t = \frac{P_t}{\Omega_t} = \frac{\pi}{2\lambda} \rho R^3 v^2 C_p \qquad (6)$$

A. Mechanical System:
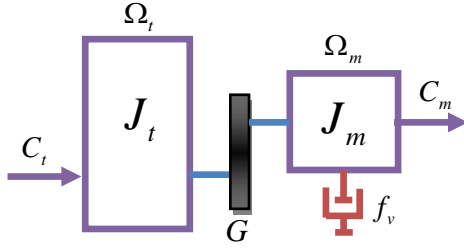Mechanical model will be represented in Figure 1

Figure 1 : Mechanical model

Where: J_t: the turbine side masses, while J_m : the electrical machine mass, G is the gearbox ratio. The generator speed and the fast shaft torque are given in:

$$\Omega_m = G\Omega_t \quad (7)$$

$$C_m = C_t / G \quad (8)$$

Next,

$$C_m - C_{em} = \left(\frac{J_t}{G^2} + J_m\right)\frac{d\Omega_m}{dt} + f_v\Omega_m \quad (9)$$

B. Maximum Power Tracking MPPT

Aiming to extract the supreme power is the fundamental objective of the speed control. Many methods are used to ensure that [25, 26]. Direct speed controller (DSC) is presented in fig 2, its concept is founded on generating the optimal turbine speed for various wind speed value, and use it as speed reference. Next, with the help of a regulator the turbine rotational speed is controlled and the mechanical power aimed to be maximal for each operating point; the reference rotational speed is defined by:

$$\Omega_t^* = (\lambda_{opt}v)/R \quad (10) \quad \text{Thus,} \quad \Omega_m^* = G\Omega_t^* \quad (11)$$
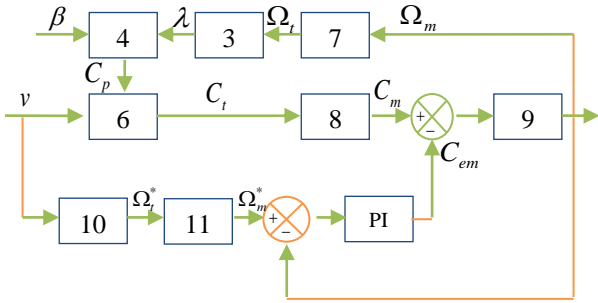

Figure 2 :Direct speed control.

We obtain the active power reference by the following equation:

$$P_{s\_ref} = C_{cem\_ref}\Omega_m \quad (12)$$

III. MATHEMATICAL MODEL OF DFIG:

We have chosen to use the double-fed induction generator because with the help of the bi-directional converter working in both super-synchronous and sub-synchronous is possible. The electrical model is obtained using Park transformation is given by [24, 26, 27]:

Stator, rotor voltages: Eqts (13-16)

$$xV_{qs} = R_sI_{qs} + \frac{d\phi_{qs}}{dt} - \omega_s\phi_{ds} \; ; \; V_{ds} = R_sI_{ds} + \frac{d\phi_{ds}}{dt} - \omega_s\phi_{qs}$$

$$V_{dr} = R_rI_{dr} + \frac{d\phi_{dr}}{dt} - \omega\phi_{qr} \; ; \; V_{qr} = R_rI_{qr} + \frac{d\phi_{qr}}{dt} - \omega\phi_{dr}$$

Where: $\omega = \omega_s - \omega_m \quad (17)$

Stator, rotor fluxes:

$$\phi_{ds} = L_sI_{ds} + MI_{dr} \quad (18) \qquad \phi_{qs} = L_sI_{qs} + MI_{qr} \quad (19)$$

$$\phi_{dr} = L_rI_{dr} + MI_{ds} \quad (20) \qquad \phi_{qr} = L_rI_{qr} + MI_{qs} \quad (21)$$

The electromagnetic torque is:

$$C_{em} = P\left(\phi_{ds}I_{qs} - \phi_{qr}I_{ds}\right)$$
$$= PM\left(I_{dr}I_{qs} - I_{qr}I_{ds}\right) \quad (22)$$

The motion equation is:

$$C_{em} - C_r = J\frac{d}{dt}\Omega_m + f_v\Omega_m \quad (23) \quad J = \frac{J_{turbine}}{G^2} + J_g \quad (24)$$

Where: the load torque is C_r, J is inertia in generator rotor, mechanical speed is Ω_r.

IV. THE DFIG VECTOR CONTROL:

In this section, the application of vector control DFIG is to achieve a decoupling between the quantities generating torque and flux. For this, we adjust the flux by (I_{ds} or I_{dr}), and torque by (I_{qs} or I_{qr}). Thus, the dynamics of DFIG will be reduced to that of a DC machine. This method can be outlined as shown in Fig 3.
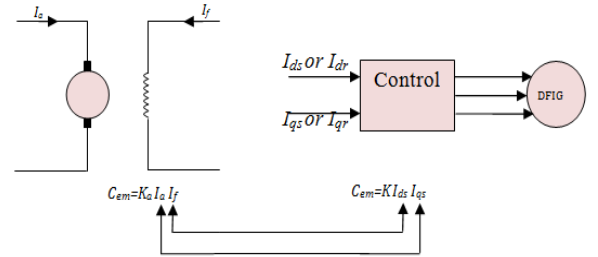

Figure 3 : Analogy between the vector control of DFIG and the control of a DC machine.

The DFIG model can be uttered in the synchronous frame as shown in fig. 4 by: ($\phi_{ds} = \phi_{qs}$) and ($\phi_{qs} = 0$) [7, 24, 26, 28]. By neglect stator resistances voltage will be:

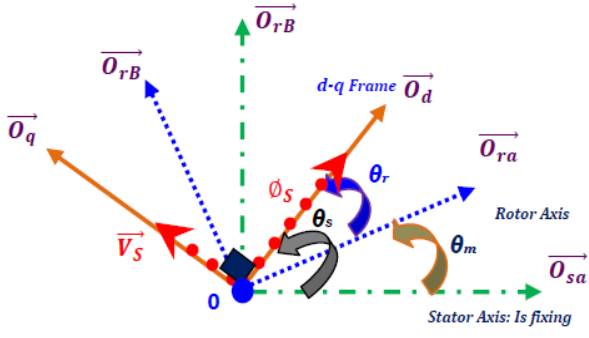$$V_{ds} = 0 \text{ and } V_{qs} = V_s = \omega_s\phi_s \quad (25)$$

Figure 4 : Stator and rotor flux vectors.

We drive to an uncoupled power control; where, I_{dr} controls the active power, the reactive power is controlled by the direct component I_{ds} [29] as presented in fig. 5:

$$P_s = -V_s \frac{M}{L_s} I_{qr} \quad (26)$$

$$Q_s = \left(\frac{\phi_s V_s}{L_s} - \frac{M}{L_s} V_s I_{dr} \right) \\ = \left(\frac{V_s^2}{\omega_s L_s} - \frac{M}{L_s} V_s I_{dr} \right) \quad (27)$$

The equations of the voltages according to the rotor currents are shown below (fig. 5):

$$V_{dr} = R_r I_{dr} + L_r \sigma \frac{dI_{dr}}{dt} - L_r \sigma \omega I_{qr} \quad (28)$$

$$V_{qr} = R_r I_{qr} + L_r \sigma \frac{dI_{qr}}{dt} - L_r \sigma \omega I_{dr} + \frac{M}{L_s} \omega \phi_s \quad (29)$$

With: $\qquad \sigma = \left(1 - M^2\right)/L_s L_r \quad (30)$

Where: V_{dr}, V_{qr} are rotor voltage; R_r is the rotor resistances; L_r, L_s are the rotor inductances; M is mutual inductance; σ is leakage factor.
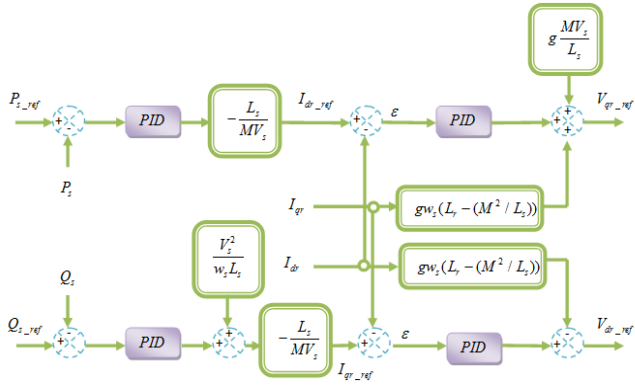

Figure 5 : Power Control.

V. THE BASIC PRINCIPLE OF HIS-PID

The basic of HSIC is to produce the control action according to the current and the former control experiences which means it can recognize and utilize the information character provided by control system dynamic process furthest, embarking on enlighten and intuitive detection and thus implementing the effect control of object without the precise mathematic model. The prime goal of HSIC is not the control object but how controller itself simulates controller's construction and behavior function, the human controller produces a large control action to restrain the error; when the error is large, the HISC produces an inaccuracy control action, however when the error minimized, the HISC will steadily reduce the control action to limit the degressive rate of error and tend to prevent the overshoot; if the error is too small, the HISC produces a precise control action ,the control amplitude is specified by the size of error and tendency that the error is changing. Based on the report above, it is easy to see that the HIS law is in a good agreement with the sigmoid-type function [21, 30, 31].

The main objective of the HIS-PID is to reduce the error and making it change along the desired law even with disturbances; HIS-PID is a procedure of automatically accumulating the control experiences, self-adapting of all kinds of disturbances and uncertainties [30]. The integral action must be introduced into the control law, as follows:

$$\begin{cases} u = k_m \ddot{e}_{max} \, sigmoid\left(\dfrac{-k_p\left(\tilde{\tilde{e}} + k_d \dot{e} \right)}{\tilde{\tilde{e}}_{max}} \right) + k_i \sigma \\ \dot{\sigma} = k_m \ddot{e}_{max} \, sigmoid\left(\dfrac{-k_p\left(\tilde{\tilde{e}} + k_d \dot{e} \right)}{\tilde{\tilde{e}}_{max}} \right) \end{cases} \quad (31)$$

$$\begin{cases} u = k_m \ddot{e}_{max} \, sigmoid\left(\dfrac{-k_p\left(\tilde{\tilde{e}} + k_d \dot{e} \right) - k_i \sigma}{\tilde{\tilde{e}}_{max}} \right) \\ \dot{\sigma} = \tilde{\tilde{e}} + k_d \dot{e} \end{cases} \quad (32)$$

Where k_i , k_p, k_d ,k_m , $\ddot{e}_{max}$ are a positive constants. $\tilde{\tilde{e}}$ is Tow error and it is defined by :

$$\tilde{\tilde{e}} = \begin{cases} \tilde{\tilde{e}}_{max} & e \geq \tilde{\tilde{e}}_{max} \\ e & -\tilde{\tilde{e}}_{max} \prec e \prec \tilde{\tilde{e}}_{max} \\ -\tilde{\tilde{e}}_{max} & e \leq \tilde{\tilde{e}}_{max} \end{cases} \quad (33)$$

The main features of the control laws (31) and (32) are:
➤ The integrator output remains constant when $\tilde{\tilde{e}} + k_d \dot{e} = 0$.
➤ Combine and use the prior knowledge.

➢ Rapid adaptive or self-learning ability, better flexibility, stronger robustness.

In Order to improve the HIS-PID we will use the hyperbolic tangent function in order to smooth the control signal, the function is shown in Figure 6 and it's defined by:

$$U_n = K \frac{S(x)}{|S(x)| + \delta} + \eta \qquad (34)$$

Thus,

$$\delta = \begin{cases} \delta_0 & \text{if } |S(x)| \geq \varepsilon \\ \delta_0 + \gamma \int S(x) dt & \text{if } |S(x)| \prec \varepsilon \end{cases} \qquad (35)$$

$$\eta = \begin{cases} 0 & \text{if } |S(x)| \geq \varepsilon \\ \xi \int S(x) dt & \text{if } |S(x)| \prec \varepsilon \end{cases} \qquad (36)$$

Where: $\delta, \eta, \xi, \varepsilon, \gamma$ are positive constants.
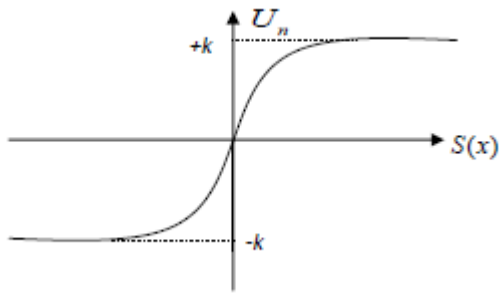
Figure 6 : hyperbolic tangent function.

VI.   SIMULATION RESULTS

In this section, simulation tests have been performed with the help of Matlab. DFIG performance will be compare with two different controllers. The PI and the HIS-PID will be tested and compared

Reference tracking

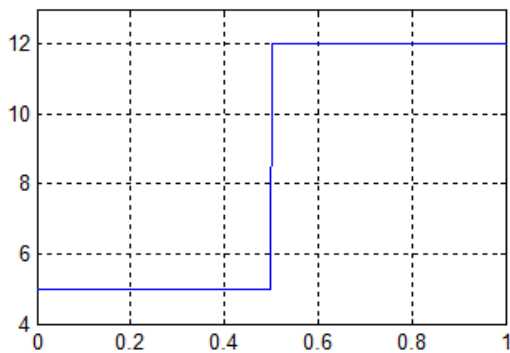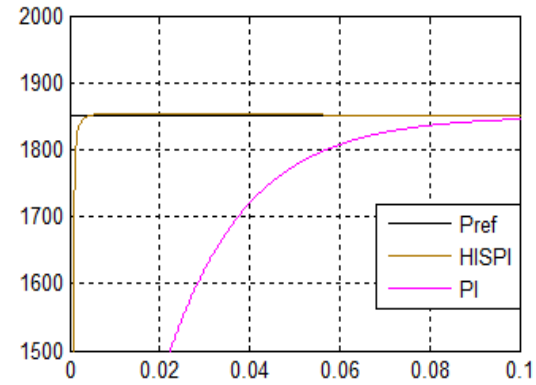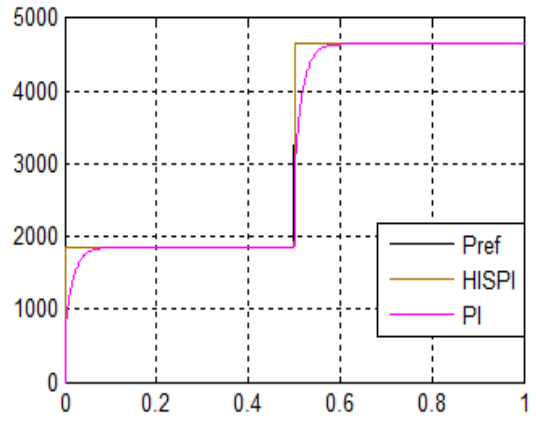Wind speed shown in Fig (7, 11) in order evaluates the designed control.

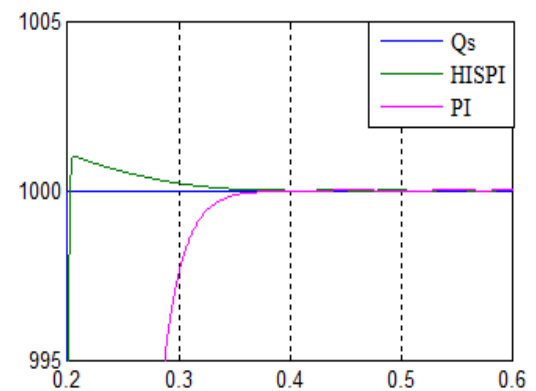Figure 7 : Wind speed
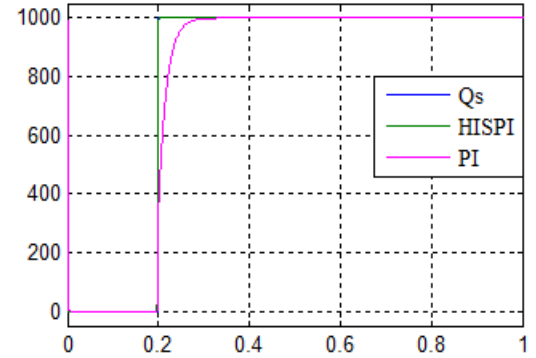

Figure 8 : Stator Active power Ps

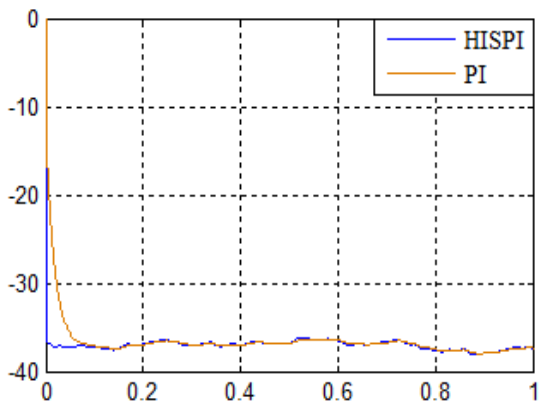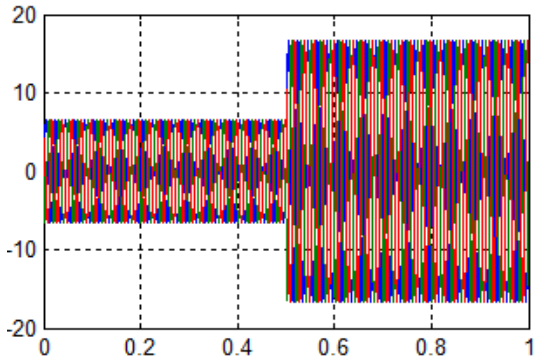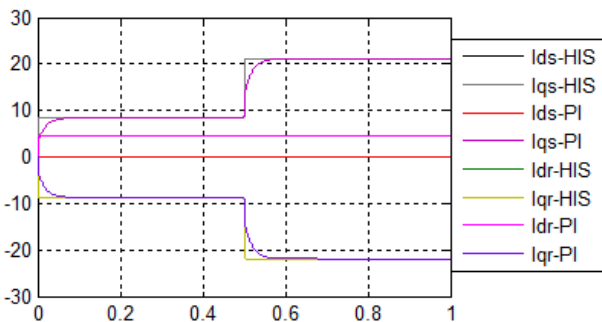
Figure 9 : Reactive Active power Qs

A

B

C

Figure 10 : A- Electromagnatique couple B- Stator current
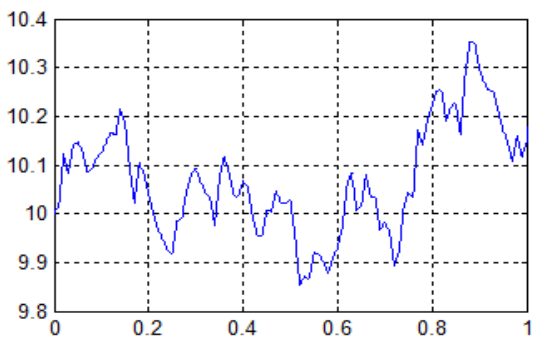C- stator and otor current components

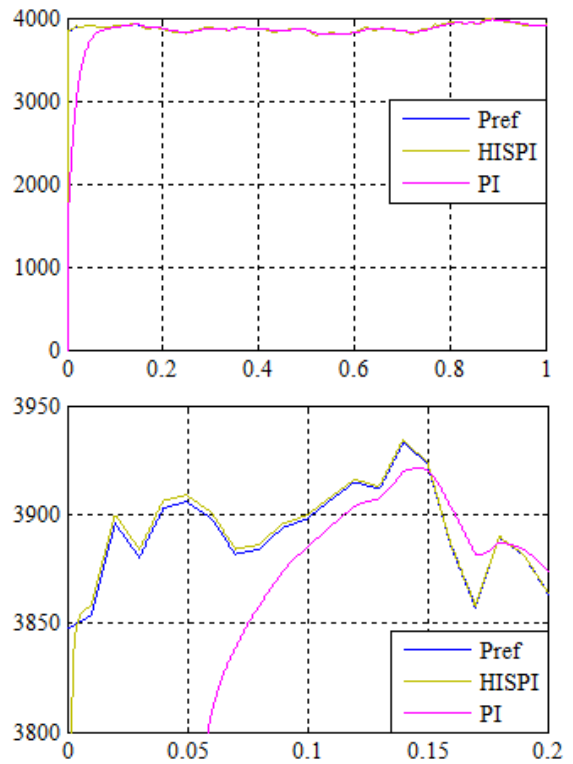

Figure 11 : Wind speed

Figure 12 : Stator Active power Ps
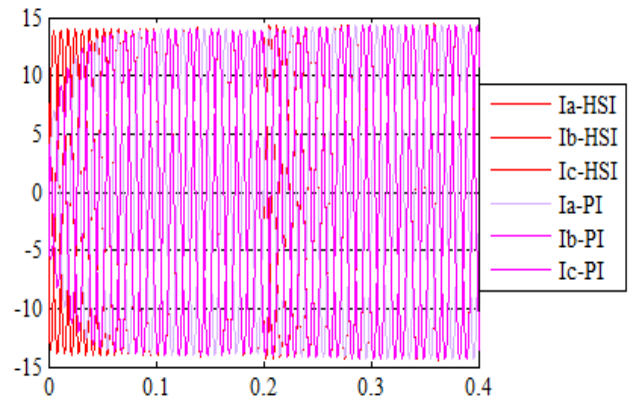
Figure 13 : Stator current

The electromagnetic torque is shown in Fig (10-A) is negative due to the generator operation. A very good decoupling between the two components of the rotor and stator current is obtained as shown in fig 10-C ensuring a decoupled control of powers Fig 8, 9 and 12 represent the stator active and reactive powers and its reference profiles using PID regulator and HIS-PID, we can notice that the dynamic response of the stator active power and reactive power under HIS-PID control is much faster than that under the conventional PID control and it track almost perfectly their references. This outcome tends to guarantee stability and the power quality even when there is a change in wind speed.

VII. CONCLUSION

In this article, a complete system to produce electrical energy with a doubly fed induction generator in wind turbine, incorporating a maximum power point tracker for dynamic power control has been presented. Control of the machine inverter provides a set of active and reactive powers exchanged between the grid and the machine. With the consideration of turbine variable velocity state and design controller for DFIG in form of using Human Simulating Intelligent PID Control was proposed, simulation results show that the proposed controller provides a notable efficiency, since it permits to track the optimum power quickly despite the speed wind changing. On the other hand, the stator power quantities show smooth waveforms, with great tracking indices. Consequently, undesirable mechanical stresses are avoided

APPENDIX

The generator's parameters are presented below:
$R_s = 1.2\Omega$, $R_r = 1.8\Omega$, $L_s = 0.1554H$, $L_r = 1.558$ H, $M = 0.15$, $V_s = 380$ V/220V; $P = 2$, $F_r = 0.0027$N.s/rad, $f = 50$Hz; $J = 0.042$ kg.m2, Aerodynamic coefficients $C1 = 0.5$, $C2 = 116$, $C3 = 0.4$, $C4 = 0$, $C5 = 5$, $C6 = 21$, controller parameter:

$$K_p = \frac{t_r}{L_r}, \; K_i = \frac{K_p R_r}{L_r \sigma}, \; K_{p\_Ir} = \frac{L_s L_r \sigma}{M V_s t_r},$$

$$K_{i\_Ir} = \frac{K_{p\_Ir} R_r}{L_r \sigma}$$

Refrences

[1] Kassem, Ahmed M., Khaled M. Hasaneen, and Ali M. Yousef. "Dynamic Modeling and Robust Power Control of Dfig Driven by Wind Turbine at Infinite Grid." International Journal of Electrical Power & Energy Systems 44, no. 1 (2013/01/ 2013): 375-82. http://dx.doi.org/http://dx.doi.org/10.1016/j.ijepes.2011.06.038.

[2] Saad, Naggar H, Ahmed A Sattar, and Abd El-Aziz M Mansour. "Low Voltage Ride through of Doubly-Fed Induction Generator Connected to the Grid Using Sliding Mode Control Strategy." Renewable Energy 80 (2015): 583-94.

[3] Phan, Dinh Hieu and ShouDao Huang. "Super-Twisting Sliding Mode Control Design for Cascaded Control System of Pmsg Wind Turbine." Journal of Power Electronics 15, no. 5 (2015): 1358-66.

[4] Jadhav, H. T. and Ranjit Roy. "A Comprehensive Review on the Grid Integration of Doubly Fed Induction Generator." International Journal of Electrical Power & Energy Systems 49 (7// 2013): 8-18. http://dx.doi.org/https://doi.org/10.1016/j.ijepes.2012.11.020.

[5] Abdeddaim, S and A Betka. "Optimal Tracking and Robust Power Control of the Dfig Wind Turbine." International Journal of Electrical Power & Energy Systems 49 (2013): 234-42.

[6] López, Eva Centeno and Jonas Persson. "High-Order Models of Doubly Fed Induction Generators." In Wind Power in Power Systems, 849-64: John Wiley & Sons, Ltd, 2012.

[7] Yamamoto, M. and O. Motoyoshi. Active and Reactive Power Control of Doubly-Fed Wound Rotor Induction Generator. 21st Annual IEEE Conference on Power Electronics Specialists, 1990.

[8] Li, H. and Z. Chen. "Overview of Different Wind Generator Systems and Their Comparisons." IET Renewable Power Generation 2, 2 (2008): 123-38. http://digital-library.theiet.org/content/journals/10.1049/iet-rpg_20070044.

[9] Hansen, Anca, Poul Sø rensen, Fredje Blaabjerg, and Florin Iov. "{Centralised Power Control of Wind Farm with Doubly Fed Induction Generators}." Renewable Energy 31, no. 7 (June// 2006): 935-51. http://dx.doi.org/citeulike-article-id:8373947

doi: 10.1016/j.renene.2005.05.011.

[10] Caliao, Nolan D. "Dynamic Modelling and Control of Fully Rated Converter Wind Turbines." Renewable Energy 36, no. 8 (8// 2011): 2287-97. http://dx.doi.org/https://doi.org/10.1016/j.renene.2010.12.025.

[11] Taveiros, F. E. V., L. S. Barros, and F. B. Costa. "Back-to-Back Converter State-Feedback Control of Dfig (Doubly-Fed Induction Generator)-Based Wind Turbines." Energy 89 (9// 2015): 896-906. http://dx.doi.org/https://doi.org/10.1016/j.energy.2015.06.027.

[12] Qiao, W. Dynamic Modeling and Control of Doubly Fed Induction Generators Driven by Wind Turbines. 2009 IEEE/PES Power Systems Conference and Exposition, 2009.

[13] Ahmed, T., K. Nishida, and M. Nakaoka. "A Novel Stand-Alone Induction Generator System for Ac and Dc Power Applications." IEEE Transactions on Industry Applications 43, no. 6 (2007): 1465-74. http://dx.doi.org/10.1109/TIA.2007.908210.

[14] Lopez, J., P. Sanchis, X. Roboam, and L. Marroyo. "Dynamic Behavior of the Doubly Fed Induction Generator During Three-Phase Voltage Dips." IEEE Transactions on Energy Conversion 22, no. 3 (2007): 709-17. http://dx.doi.org/10.1109/TEC.2006.878241.

[15] Alaya, J. B., A. Khedher, and M. F. Mimouni. Nonlinear Vector Control Strategy Applied to a Variable Speed Dfig Generation System. Eighth International Multi-Conference on Systems, Signals & Devices, 2011.

[16] Shtessel, Y., C. Edwards, L. Fridman, and A. Levant. Sliding Mode Control and Observation. Springer New York, 2013.

[17] Song, Zhanfeng, Tingna Shi, Changliang Xia, and Wei Chen. "A Novel Adaptive Control Scheme for Dynamic Performance Improvement of Dfig-Based Wind Turbines." Energy 38, no. 1 (2012/02/01/ 2012): 104-17. http://dx.doi.org/http://dx.doi.org/10.1016/j.energy.2011.12.029.

[18] Zhi, D., L. Xu, and John A. Morrow. Improved Direct Power Control of Doubly-Fed Induction Generator Based Wind Energy Generation System. 2007.

[19] Slotine, J.J.E. and W. Li. Applied Nonlinear Control. Prentice-Hall, 1991.

[20] Yang, Bo, Lin Jiang, Lei Wang, Wei Yao, and Q. H. Wu. "Nonlinear Maximum Power Point Tracking Control and Modal Analysis of Dfig Based Wind Turbine." International Journal of Electrical Power & Energy Systems 74 (1// 2016): 429-36. http://dx.doi.org/https://doi.org/10.1016/j.ijepes.2015.07.036.

[21] Feng-rui, Z. and H. Da-yong. Research of Human-Simulated Intelligent Controller in Industrial Control. Vol. 3. 2010 Second International Workshop on Education Technology and Computer Science, 2010.

[22] Liu, Shu-Jun, XH Gai, and NL Zhang. "Research and Simulation of Anti-Disturbance Problem on Improved Characteristic Model Algorithm of Hsic [J]." Journal of System Simulation 20, no. 11 (2008): 2905-08.

[23] Zeng, J, XM Sun, and NL Zhang. A New Type of Nonlinear Controller-Nine-Point Controller [C]. Proceedings of the 2002 International Conference on Control and Automation, 2002.

[24] Abad, Gonzalo, Jesús López, Miguel A. Rodríguez, Luis Marroyo, and Grzegorz Iwanski. "Direct Control of the Doubly Fed Induction Machine." In Doubly Fed Induction Machine, 363-477: John Wiley & Sons, Inc., 2011.

[25] Aimani, S.E. Modélisation Des Différentes Technologies D'éoliennes Intégrées Dans Un Réseau De Moyenne Tension. 2004.

[26] Poitiers, Frédéric. "Etude Et Commande De Generatrices Asynchrones Pour L'utilisation De L'energie Eolienne
 - Machine Asynchrone À Cage Autonome
 - Machine Asynchrone À Double Alimentation Reliée Au Réseau." Université de Nantes, 2003. Univ-nantes Univ-nantes-theses. https://tel.archives-ouvertes.fr/tel-00011383.

[27] Lie, Xu and P. Cartwright. "Direct Active and Reactive Power Control of Dfig for Wind Energy Generation." IEEE Transactions on Energy Conversion 21, no. 3 (2006): 750-58. http://dx.doi.org/10.1109/TEC.2006.875472.

[28] Rahimi, Mohsen and Mostafa Parniani. "Dynamic Behavior Analysis of Doubly-Fed Induction Generator Wind Turbines – the Influence of Rotor and Speed Controller Parameters." International Journal of Electrical Power & Energy Systems 32, no. 5 (6// 2010): 464-77. http://dx.doi.org/https://doi.org/10.1016/j.ijepes.2009.09.017.

[29] Jemmli, K, Mohamed Jemli, Moncef Gossa, and Mohamed Boussak. "Power Flow Control and Var Compensation in a Doubly Fed Induction Generator." International Journal of Sciences and Techniques of Automatic control & computer engineering, Special issue CEM (2008): 548-65.

[30] Liu, Zhuning. "Human-Simulating Intelligent Pid Control." International Journal of Modern Nonlinear Theory and Application 6, no. 02 (2017): 74.

[31] Tang, Wei and Hao Cheng. Design of Human-Simulation Intelligent Pid Based on Apmp Refiner Control. Vol. 591. Advanced Materials Research: Trans Tech Publ, 2012.